HHS Public Access

Author manuscript

Anat Rec (Hoboken). Author manuscript; available in PMC 2019 October 18.

Published in final edited form as:

Anat Rec (Hoboken). 2019 October ; 302(10): 1754–1769. doi:10.1002/ar.24139.

Anatomical Assessment of the Adult Skeleton of Zebrafish Reared Under Different Thyroid Hormone Profiles

STEPHANIE KEER[1], **KARLY COHEN**[1], **CATHERINE MAY**[2], **YINAN HU**[2], **SARAH McMENAMIN**[2,*], **LUZ PATRICIA HERNANDEZ**[1,*]

[1]Department of Biological Sciences, The George Washington University, Science and Engineering Hall, Washington, District of Columbia

[2]Biology Department, Boston College, Chestnut Hill, Massachusetts

Abstract

Thyroid hormone (TH) directs the growth and maintenance of tissues throughout the body during development and into adulthood, and plays a particularly important role in proper ossification and homeostasis of the skeleton. To better understand the roles of TH in the skeletogenesis of a vertebrate model, and to define areas of the skeleton that are particularly sensitive to developmental TH, we examined the effects of hypo-and hyperthyroidism on skeletal development in zebrafish. Performing a bone-by-bone anatomical assessment on the entire skeleton of adult fish, we found that TH is required for proper ossification, growth, morphogenesis, and fusion of numerous bones. We showed that the pectoral girdle, dermatocranium, Weberian apparatus, and dentary are particularly sensitive to TH, and that TH affects development of skeletal element regardless of bone type and developmental origin. Indeed, the hormone does not universally promote ossification: we found that developmental TH prevents ectopic ossification in multiple thin bones and within connective tissue of the jaw. In all, we found that TH regulates proper morphogenesis and ossification in the majority of zebrafish bones, and that the requirement for the hormone extends across bone types and developmental profiles.

Keywords

hypothyroidism; hyperthyroidism; skeletogenesis; ossification; craniofacial

INTRODUCTION

Hypo-and hyperthyroidism can be caused by a variety of disorders (Devdhar et al., 2007; Persani, 2012; De Leo et al., 2016), and cause wide-ranging systemic effects in vertebrates. In particular, well-regulated thyroid hormone (TH) titer is critical for normal skeletal development. In mammals, hypothyroidism impairs linear growth, delays endochondral ossification, and reduces mineralization while hyperthyroidism leads to osteoporosis, early

*Correspondence to: Sarah McMenamin, Biology Department, Boston College, Chestnut Hill, MA 02467. E-mail: mcmenams@bc.edu; and Luz Patricia Hernandez, Department of Biological Sciences, The George Washington University, Science and Engineering Hall, Washington, DC 20052. phernand@gwu.edu.

Additional Supporting Information may be found in the online version of this article.

fusion of bones, and increased mineral deposition (Devdhar et al., 2007; Persani, 2012; Bassett and Williams, 2016; De Leo et al., 2016). Furthermore, aberrant TH titer is associated with bone density alterations and increased risk of bone fracture (Vestergaard and Mosekilde, 2002; Vestergaard et al., 2005). Thus, understanding the roles that TH plays in bone development and homeostasis is of interest to both basic skeletogenesis and biomedicine.

Studies in mammals and mammalian cells show that, in general, TH promotes ossification and regulates the transition between chondrogenesis and osteogenesis. In endochondral bone, TH inhibits chondrocyte proliferation, inducing hypertrophic differentiation to promote cartilage mineralization and the transition into osteogenesis (Ishikawa et al., 1998; Robson et al., 2000; Miura et al., 2002; Lassova et al., 2009). The hormone subsequently induces apoptosis of hypertrophic chondrocytes and stimulates vascularization of the newly mineralized tissue (Ducy et al., 1997; Himeno et al., 2002; Kronenberg, 2003; Makihira et al., 2003). Vascularization ultimately attracts osteoblasts into the cartilaginous scaffold and allows mineralization. Osteoblast responses to TH are highly context-dependent, but the hormone generally stimulates synthesis of bone matrix (Klaushofer et al., 1989; Fratzl-Zelman et al., 1997; Gouveia, 2001; O'Shea et al., 2012). The hormone also increases activity of bone-degrading osteoclasts (Mundy et al., 1976; Allain and McGregor, 1993; Bassett and Williams, 2016). While TH is critical for ossification in numerous contexts, the role of the hormone in patterning bones is not well understood. Further, we lack an adequate understanding of how the hormone affects different skeletal elements and different types of bones across the body.

Here, we use the zebrafish as a model to better understand the roles of TH in bone development and homeostasis. Zebrafish have emerged as a premier model organism with an abundance of transgenic and genetic tools and imaging capabilities. In addition to being a biomedically relevant model, zebrafish are also a member of Cypriniformes, a diverse order of more than 3,200 species that dominate freshwaters across the globe (Nelson, 2006). Ostariophysi, the larger group that includes Cypriniformes, has a number of evolutionary novelties including the Weberian apparatus (bony ossicles that connect the swim bladder to the inner ear, making species within this group hearing specialists) (Bird and Hernandez, 2007; Hernandez et al., 2007). Cypriniformes in particular possess the kinethmoid, a sesamoid bone that mediates premaxillary protrusion (Hernandez et al., 2007; Hernandez and Staab, 2015).

Previous work on zebrafish has shown that TH affects the Weberian apparatus, supraneurals, some craniofacial features, and the neural and hemal arches and spines (Shkil et al., 2012; Kapitanova and Shkil, 2014a,b), although no comprehensive study of all skeletal elements has been performed. Work in barbs, another cypriniform group, has shown that the ossification sequence of cranial bones changed during ontogeny under different TH conditions (Shkil et al., 2010a). Since TH modulation can produce suites of coordinated morphological changes, the hormone is a potential target for adaptation and diversification in fishes and other vertebrates; a better understanding of the skeletal modules regulated by the hormone can lend insight into TH as a target for evolutionary adaptation.

In this study, we answer two overarching questions about the roles of TH in skeletogenesis: (1) Which bones require TH for proper ossification and morphogenesis? and (2) Do bones with different developmental origins or profiles have particular sensitivities to TH? We anticipate that the comprehensive anatomical atlas presented will facilitate further investigation into the roles of TH in vertebrate (and particularly cypriniform) skeletogenesis, and that it will further serve as a reference for normal zebrafish skeletal anatomy.

METHODS AND MATERIALS

Thyroid Ablation and Fish Husbandry

All research was performed in accordance with protocols approved by the Institutional Animal Care and Use Committee of Boston College: Institutional Animal Welfare Number Assurance Identification D16–00521; Protocol 2007–006–01. Euthyroid and hypothyroid *Tg(tg:nVenus-2a-nfn)*$^{wp.rt8}$ line (McMenamin et al., 2014). As detailed in McMenamin et al. (2014), 4 dpf transgenic fish were incubated overnight with either 10-mM metronidazole + 1% DMSO to induce thyroid ablation (hypothyroid condition) or with 1% DMSO alone (euthyroid condition). Metronidazole-treated fish were examined after ablation to ensure nVenus expression was no longer present. These thyroid-ablated, hypothyroid fish are hereafter referred to as TH−; their DMSO-treated euthyroid controls are referred to as WT. *opallus* mutant fish show constitutive hyperthyroidism (McMenamin et al., 2014), and are hereafter referred to as TH+. All fish were reared under standard conditions (28 degree, 12:12 light cycles), recirculating water was carbon-filtered, and fish were fed TH-free food: rotifers fed with RotiGrow Plus (Reed Matriculture), *Artemia,* and pure Spirulina flakes (Pentair).

Clearing and Staining

Fish were collected between 20 and 23 mm standard length (SL) and preserved in 4% PFA. Specimens were cleared and stained according to a modified Walker and Kimmel (2007) protocol (N = 12 per TH condition).

Histology

Adult *Danio rerio* specimens (>20 mm SL) from each of the three thyroid treatments (N = 4 per TH condition) were infiltrated and subsequently embedded in a JB-4 solution following the Electron Microscopy Science JB-4 Embedding media protocol. Specimens were sectioned sagittally. Histological sections were taken at 2 μm and stained with Lee's Methylene Blue-Basic Fuchsin stain.

Scoring and Statistics

In order to determine if different categories of bones showed specific sensitivities to TH, every bone was given a score from 1 to 3 (1 being unaffected; 3 being severely affected) for degree of ossification and for shape, both with reference to the control WT fish. For the sake of consistency, all scoring was performed by a single individual and then rechecked by a second individual.

Bones were sorted into categories based on their embryonic germ layer origins (derived from mesoderm or from neural crest cells [NCC]) and development type (dermal or endochondral; based on Cubbage and Mabee, 1996; Bird and Mabee, 2003). Bone names as well as size (SL) at which each bone ossified were based on Cubbage and Mabee, 1996; Bird and Mabee, 2003. Craniofacial bones were sorted based on whether they were cellular, compact, spongy, and/or tubular (based on Weigele and Franz-Odendaal, 2016).

All statistical analyses were performed in R (version 3.4.4). Correlations among shape and ossification scores of different TH backgrounds were assessed by Kendall's rank correlation via the cor.test function from package "stats." To assess how location (craniofacial vs. axial), developmental origin (germ layer; dermal vs. endochondral), developmental timing (body size at the onset of ossification), and bone type (cellular; compact; tubular; spongy) may affect shape and ossification score, we built ordinal logistic regression models via the polr function from package "MASS." McFadden pseudo-R^2 values associated with each model were calculated *via* the PseudoR2 function from package "DescTools" as approxies for effect size. Since multiple hypotheses were tested on the same data set, we followed the Bonferroni correction method and set the significant *P*-value threshold at 0.004.

RESULTS

There were numerous significant changes in skeletal structure between different TH-modified conditions relative to WT zebrafish, with TH− fish in particular showing severe and widespread skeletogenic defects. Relative to reference WT fish, the TH− skeleton was more cartilaginous overall, and the pectoral girdle, dermatocranium, and Weberian apparatus showed the most severe shape changes. Compared with WT, the TH+ skeleton was over-ossified, and the dentary and Weberian apparatus show the most significant aberrations. Systematic, qualitative comparisons between anatomical structures are described below in the order of most affected to least affected in TH− condition. To facilitate comparisons, WT anatomy is described first in each section, as per Cubbage and Mabee (1996) and Bird and Mabee (2003).

Pectoral Girdle

While the pectoral girdle supports the pectoral fins of zebrafish, the scapula and coracoid are considered homologous with those of mammals. Starting from the point of connection between the skull and the pectoral girdle, and moving ventrally are the paired posttemporals, supracleithra, cleithra (cl), coracoids (co), mesocoracoids (mco), and scapulae (sca) (Fig. 1). There are four proximal radials (rad I–IV) on each side that articulate with the scapulae. Six to seven distal radials articulate with the proximal radials and support the lepidotrichia. The paired postcleithra sit medial to the cleithra. The pectoral girdle showed significant anatomical changes under TH− development, while it appeared to be relatively unaffected by TH+ development (Fig. 1).

The proximal and distal radials are perichondral mesoderm-derived bone. In WT, the proximal radials ossify except at the distal tips of proximal radials 2, 3, and 4, which often remain cartilaginous (Fig. 1A). The distal radials ossify from a common cartilage, and cartilage often remains at the articulation point between the proximal and distal radials (see

blue at tips of rad I–IV, Fig. 1A). In TH−, the proximal radials rarely ossify; although when ossification is observed, it is usually around the midpoint of some or all of the proximal radials (Fig. 1D, circle). Ossification is also usually bilaterally asymmetric: in Figure 1D, the right proximal radial has traces of cartilage, while the left side has no such ossification. Furthermore, the cartilage of the proximal radials is frequently mispatterned, as seen in Figure 1(D) between proximal radials 3 and 4, where additional cartilage is present (Fig. 1D, asterisk). The distal radials also remain completely cartilaginous, but the articulation with the lepidotrichia remains unaffected (Fig. 1D). In the TH+ condition, the proximal and distal radials ossify normally (Fig. 1G).

The scapula, mesocoracoid, and coracoid are endochondral mesoderm-derived bones. In WT, the anterior coracoid and posterior scapula arise from the same cartilage, which ossify and fuse with each other as well as with the ventral surface of the cleithrum (Fig. 1C). There are two foramina, the coracoid foramen (cf) at the anterior of the coracoid, and the scapular foramen (sf) in the scapula where the scapula and cleithrum meet. The mesocoracoid is a thin, rodlike bone that fuses with the dorsal arm of the cleithrum, where the scapula and coracoid meet. In TH−, the coracoid and scapula fail to both properly ossify and fuse with each other and the cleithrum (Fig. 1D,F). There are often traces of cartilage around the coracoid foramen as well, although the location of that cartilage varies (Fig. 1F, asterisk). The cartilage around the scapular foramen generally ossifies completely, but when cartilage is present around the perimeter of the scapular foramen, the location of the cartilage can also vary. Both the coracoid foramen and scapular foramen are frequently irregularly shaped and are larger than in WT. The mes-ocoracoid is cartilaginous where it fuses to the scapulocoracoid and cleithrum. In TH+, the coracoid and scapula have robust ossification and are larger than that in WT, while the coracoid and scapular foramen are generally smaller than that in WT (Fig. 1I). The mes-ocoracoid is also more robust in TH+ than WT.

The cleithrum, supracleithrum, posttemporal, and postcleithrum are dermal mesoderm-derived bone. In WT, the cleithrum has a dorsal arm lateral to the skull and a ventral arm ventral to the operculum (Fig. 1A,C). The dorsal arm is ligamentously held to the supracleithrum, while the ventral arm fuses with the coracoid, mesocoracoid, and scapula. The dorsal arm of the cleithrum has a narrow tip that broadens along the anterior–posterior axis into a laterally flattened plate with a rounded posterior edge (Fig. 1C). The ventral arm of the cleithrum is another flattened plate that curves anteromedially to a tip that meets at the midline (Fig. 1 (A)). In TH−, the cleithrum is fused with the coracoid, mesocoracoid, and scapula, but the dermal bone does not ossify in the correct shape (Fig. 1D). The anteromedial aspect of the ventral arm is foreshortened compared with WT, and rectangular rather than curved (Fig. 1D, enclosed in rectangle). The angle at which the lateral and ventral arms meet is more obtuse as well. In TH+, the cleithrum has ossified in the correct shape but is overall more robust (Fig. 1G,I). The anteromedial aspect of the ventral arm is more curved than in WT (Fig. 1G). In addition, the angle at which the lateral and ventral arms meet is also more obtuse in TH+.

In WT, the postcleithrum sits medial to the pectoral girdle with the dorsolateral end adjacent to the cleithrum and the ventromedial end positioned near the medial proximal radials (Fig. 1B). In TH−, the shape of the post-cleithrum is thinner, is shorter, and has secondary ossified

projections present (Fig. 1E). In TH+, the postcleithrum fuses with the cleithrum and is larger and more ossified than that in WT (Fig. 1H).

The supracleithrum and posttemporals are normal in their morphology in TH− and TH+.

Dermatocranium and Neurocranium

The zebrafish skull is composed of the dermatocranium and neurocranium. Dorsally, the dermatocranium is composed (anterior to posterior) of the paired frontals, parietals, pterotics, and supratemporals. The caudal portion of the neurocranium is composed of the occipital series: the unpaired supraoccipital, paired exoccipitals, and unpaired basioccipital. Ventrally, anterior to posterior, the neuro-cranium is composed of the paired orbitosphenoids, pterosphenoids, sphenotics, prootics, and intercalars, while the unpaired parasphenoid spans almost the entire length of the braincase at the midline. The rostral portion of the neurocranium is composed of the paired nasals, unpaired vomer, and the ethmoid series: the unpaired supraethmoid and ethmoid as well as the paired pre-ethmoids and lateral ethmoids. As seen in the pectoral girdle, TH− conditions cause more severe defects than TH+ conditions.

The frontals (f) are dermal (mesoderm-and NCC-derived) bone, while the parietals (p) are dermal (mesoderm-derived) bone, which together form the roof of the skull. In WT adults, the frontals overlap one another as well as overlap with the parietals (Fig. 2A box, B). The parietals overlap each other, the frontals rostrally, and the supraoccipital caudally (Fig. 2A box, B). The point of fusion of the frontals and parietals is marked by arrows (Fig. 2B, arrow). In TH−, the frontals fail to fuse along the midline and along the transverse axis where the frontals and parietals meet, resulting in a hole in the center of the skull roof (Fig. 2(D) box, E arrow). The unossified portion of the TH− skull is situated dorsal to the optic foramen, and so it is possible to see through the skull (in particular, observe the white space anterior to the hole labeled in Fig. 2E by the arrow). The parietals also occasionally fail to meet the supraoccipital, leaving a second more posterior hole in the skull roof. In TH+, the frontals and parietals show the opposite situation, over-lapping more than in WT (Fig. 2G box, H).

The remainder of the braincase is both dermal and endochondral bones from mesoderm-and NCC-derived populations. In WT, the pterotics and supratemporals help form the dorsal portion of the brain case; the occipital series forms the caudal portion; and the pterosphenoids, sphenoids, prootics, and intercalars form the part of the ventral portion and ossify completely and fuse with neighboring bones (Fig. 2A,C). Elements of the ethmoid series, vomer, and nasals from the rostral portion of the braincase, and the orbitosphenoids and para-sphenoid form part of the ventral portion of the braincase (Fig. 2A,C).

No element of the braincase shows the same extreme sensitivity to TH as the dermatocranium. In TH−, the endochondral bones of the braincase show increased cartilage at the junctions between bones (compare blue in Fig. 2D,F with Fig. 2A,C). Furthermore, the orbitosphenoid (os), pterosphenoid (pts), and supraorbital (so) often display signs of improper ossification, such as the presence of holes in the bone. There is less cartilage in TH

+ than in WT, and more fusion between the individual bones throughout the entire skull (compare blue in Fig. 2G,I with Fig. 2A,C).

Weberian Apparatus

The Weberian apparatus is an evolutionary novelty within the Ostariophysi (a large group of fishes comprised of catfishes, carps, minnows, loaches, etc.) that transmits sound/vibration from the swim bladder to the inner ear. Ligamentous attachments unite the anterior swim bladder to the inner ear via the mobile ossicles (these function much like mammalian ear ossicles). The Weberian apparatus is divided into the Weberian ossicles (which transfer vibrations) and the skeletal elements supporting them. From anterior to posterior, the Weberian ossicles are the paired scaphia, claustra, intercalaria, tripus, and os suspensoria. The rest of the Weberian apparatus is comprised of unpaired elements and includes the first four vertebrae (with which the ossicles articulate), first two supraneurals, and all associated processes on these vertebrae. The Weberian apparatus is sensitive to both TH− and TH+ conditions, and shows particularly severe patterning defects in TH−.

All elements of the Weberian apparatus are mesoderm-derived and are formed from a combination of endochondral and dermal bone. In WT, the scaphium has an articular process that articulates with the first vertebral centrum, a posterodorsally angled process (pap), and a concha (con) with two arches that forms the posterolateral wall of the connection to the inner ear (Fig. 3A1). The concha is medially concave and laterally convex. In TH−, the dorsal arches of the scaphium are smaller and the overall convex shape of the scaphium's concha is shallower, and in particular, the anterior edge is not fully formed (Fig. 3A2 black box). On some samples, the scaphium has secondary ossifications projecting from the posterodorsal process. In TH+, the convex shape of the concha is deeper and the posterodorsal process is more robust but the scaphium is otherwise unaffected (Fig. 3A3).

In WT, the claustrum sits dorsomedial to the scaphium. It is a triangularly shaped bone that articulates with the medial surface of the scaphium's concha (Fig. 3B1). In TH−, the claustrum is improperly ossified, especially around the dorsal edge (Fig. 3B2) where the bone is very thin. The posterior leg of the claustrum (asterisk in Fig. 3B1) is smaller or nonexistent in TH− (Fig. 3B2). Furthermore, the claustrum occasionally improperly fuses to the scaphium. In TH+, the claustrum ossifies into the correct shape although it is generally more robust (Fig. 3B3).

In WT, the intercalarium is a rodlike bone that has an articular process (ap) that articulates with the second vertebral centrum, a manubrium (mb) that projects anterolaterally between the scaphium and tripus, and an ascending process (asc)-angled posterolaterally (Fig. 3C1). In TH−, the manubrium of the intercalarium always shows some defect, being either malformed or showing secondary ossifications projecting from it (Fig. 3C2, observe that the manubrium is greatly thickened proximally and distally curved with the thickest part of the manubrium marked with a bar). The ascending process is also thicker in TH− fish (Fig. 3C2). In some specimens, the articular process is more cartilaginous or otherwise deformed (Fig. 3C2). In TH+, the manubrium is much more robust, and longer, and the ascending process is foreshortened and thicker (Fig. 3C3, observe that the thickest part of the manubrium has been marked with a bar).

In WT, the tripus has a discrete articular process (ap) that articulates with the third vertebral centrum, an anterior process (ap) that is angled toward the manubrium of the intercalarium, and a long, thin transformator process (tp) that curves medially and attaches to the anterior swim bladder (Fig. 3D1). In TH−, the tripus' posterior transformator process usually displays one or more defects, including a short transformator process, an improperly curved transformator process, or a split at the base of the transformator process to give rise to two transformator processes (Fig. 3D2, observe that the base of the transformator process is more rectangular than angular and is overall shorter in TH− than WT). The anterior process is much thinner and smaller than WT zebrafish, and lacks the square anterior most edge (Fig. 3D2). This defect is especially important, since it serves as the origin for a thick interossicular ligament that connects the ossicles and transduces sound. The anterior curve between the articular process (ap) and anterior process (ant), and the posterior curve between the articular process and the transformator process often fail to develop smooth curves (Fig. 3D2, circle), suggesting problems in proper pattern formation. The articular process is often deformed compared with WT (Fig. 3D2, observe the angle of the articular process, ap). This defect is particularly relevant given that the tripus must cleanly articulate with the vertebral centrum to transduce vibrations. The articular process tilting away from the centrum would affect hearing. In some samples, the tripus also showed signs of improper ossification that results in holes in the bone, as well as fusion to the os suspensorium.

Similar malformations are found in TH+ (Fig. 3D3). The transformator process often fails to ossify properly, resulting in long, improperly curved or split transformator processes (Fig. 3D3, observe the long transformator process). The anterior edge of the tripus is also usually deformed, overgrown with additional bone that bulges outward, and the posterior curve can be steeper than in WT(Fig. 3D3, black circle). The anterior process is smaller in TH+, although it usually maintains the square shape at the anterior-most tip (Fig. 3D3).

In WT, the os suspensoria are adjacent to the anterior swim bladder (Fig. 3E1). The os suspensoria usually fuse where they meet medially, while the lateral arms (lat) usually, but not always, have a secondary projection toward the midline. In TH−, the ossified processes are thinner and shorter, often showing greatly trabeculated bones and cartilaginous tips (Fig. 3E2, compare the blue with 3E1), and pronounced bilateral asymmetry. The midsagittal fusion fails to occur as the os suspensoria rarely develop enough to meet and usually one of the midline or lateral arms fail to develop at all (Fig. 3E2 black box). In TH+, the normal shape is maintained but the os suspensoria are larger with more robust processes (Fig. 3E3). The size, shape, and ossification of the Weberian ossicles are highly sensitive to developmental TH titer.

In WT, the remaining elements of the Weberian apparatus include the first vertebra and its lateral process, which extends laterally from the vertebra beneath the scaphium, and the second vertebra and its second lateral process, which extends laterally beneath the inter-calarium and is angled to curve around the anterior process of the tripus. Supraneurals 2 and 3 sit above vertebrae 2 and 3. In TH−, the supraneurals are more cartilaginous but the elements are otherwise unaffected. As with other elements in TH+, the supraneurals are generally larger and more robustly ossified than in WT.

Pharyngeal Jaws and Branchial Basket

The branchial basket supports the gills and comprises most of the viscerocranium. From anterior to posterior, the branchial basket is made up of elements of the hyoid arch and branchial arches I–V. The elements of the hyoid arch that make up the branchial basket are, from ventral to dorsal, the unpaired basihyal and paired dorsal and ventral hypohyals, ceratohyals, epihyals, and inter-hyals. The bones of branchial arches I–IV are, from ventral to dorsal, the unpaired basibranchial and paired hypobranchials, ceratobranchials, epibranchials, and pharyngobranchials (Fig. 4A). The bones of branchial arch V are paired enlarged ceratobranchials that serve as the pharyngeal jaws.

All elements of the branchial basket are endochondral NCC-derived bone. In WT, the pharyngeal jaws are crescent-shaped with teeth ankylosed to them and supported by bony struts (Fig. 4B, the box surrounds the teeth and the arrow points to one of the bony struts). There were an average of 9.6 fully ankylosed teeth on each pharyngeal jaw (N = 10 fish). In TH-, the pharyngeal jaws are improperly ossified, with numerous holes in the bone surrounding the teeth (Fig. 4D, arrow, observe that the struts are thinner, more numerous, and not aligned in a single direction). The angle of the anterior and posterior arm of the pharyngeal jaws is more obtuse, and the tip of the posterior process sometimes misshapen (Fig. 4D). In TH+, pharyngeal jaws are more heavily ossified where the teeth have ankylosed to the fifth ceratobranchial and have more robust struts supporting the teeth (Fig. 4F, arrow, observe that the unidirectional struts are sufficiently robust that some of them are touching each other). The perimeter of the pharyngeal jaws is not smooth (Fig. 4F). As in many other bones examined, the pharyngeal jaws are more affected by thyroid ablation than thyroid excess.

TH controls tooth number. Thyroid ablated specimens showed an average of 12.95 teeth per pharyngeal jaw, significantly more than in WT (Fig. 4G, WT vs. TH−, $P = 1.34e-05$; 10 individuals per condition). Hyperthyroid specimens showed an average of 8.1 teeth per pharyngeal jaw, significantly less than in WT (Fig. 4G, WT vs. TH+ $P = 0.0079$; eight individuals per condition). While the right and left jaws did not show significant variation within each group, TH− jaws showed overall the most variation, ranging from 9 to 17 teeth per jaw. Further-more, while the TH+ jaws had the larger ventral and smaller mediodorsal and dorsal teeth, just a fewer number of each, TH− jaws had teeth of approximately the same size in all three rows and far more of them (Fig. 4D, F, compare with 4B).

In WT, the remaining bones of the branchial basket have small cartilaginous junctions between bones and every bone ossifies (Fig. 4A). In TH−, the cartilaginous tips of each bone in the branchial basket are larger(Fig. 4B, compare the amount of blue in TH− with WT). Furthermore, basibranchial 3, pharyngobranchials 1–3, and hypobranchials 1–3 usually remain at least partially cartilaginous rather than ossifying completely (Fig. 4C). In TH+, epibranchials four are extremely small in comparison with WT but otherwise the bones of the branchial basket all ossify completely and there is the same type of small cartilaginous junctions between the bones as in WT (Fig. 4E).

The dermal urohyal and branchiostegal rays remained unaffected in TH manipulations.

Oral Jaws, Suspensorium, and Associated Elements

The oral jaws and suspensoria are composed of bones that arise from the mandibular and hyoid arches during early development. The opercular series protects the gills and the infraorbital series surrounds the eyes. These elements make up the remainder of the skull (Fig. 5A,E,I).

The upper jaw is comprised of paired premaxillae (pm) and maxillae (mx), which are dermal NCC-derived bones, and the unpaired kinethmoid (k), which is a mesoderm-derived sesamoid bone. In WT, the premaxilla has a well-defined triangular ascending process, which sits between two discrete arms of the maxilla, the ventral and anteromedially directed rostral process, and the dorsal platelike premaxillary process (Fig. 5C). The post-eroventral end of the premaxilla is thin and bladelike in WT. The maxilla, in addition to having the rostral and premaxillary processes, also has a posteroventrally directed ascending ramus that broadens slightly midway. With the mouth closed, the kinethmoid is tucked between the ascending process of the premaxillae and the ethmoid region of the neurocranium. This sesamoid bone is ovoid in shape with pronounced paired dorsolateral projections (Fig. 5C black box and full view in D).

In TH−, the ascending process of the premaxilla is shorter and more rounded than in WT zebrafish (Fig. 5G asterisk, compare the length in TH− with that in WT). The paired premaxillae also fail to properly meet at the midline, and are often crooked at the point where these bones normally abut (Fig. 5G white arrow; note that the paired premaxillae do not meet at the rostral or caudal extremes). The premaxillae also do not fit into the groove formed by the rostral and premaxillary processes of the maxilla, in part because the premaxillary and rostral processes are misshapen and foreshortened (Fig. 5G). These processes also often have improperly ossified bone as evidenced by numerous holes within the structure. Like-wise, the ascending ramus of the maxilla often contains holes. Importantly, the kinethmoid (necessary for proper jaw protrusion in cypriniforms) is usually improperly shaped with less clearly defined dorosolateral processes and a rounder rather than ovaloid shape that lacks the characteristic lateral wings of the kinethmoid (Fig. 5H, the plus marks the dorsolateral process, shorter and less defined than in WT). The kinethmoid is also improperly ossified, as it is both cartilaginous at the anterorostral and dorsocaudal points and has numerous holes in the remaining portion (Fig. 5H).

In TH+, both the premaxilla and maxilla show no obvious differences compared with WT (Fig. 5K). The kinethmoid, however, is often asymmetrical, with one of the lateral wings often failing to grow properly, although it does ossify overall (Fig. 5L). Patterning in the premaxilla and kinethmoid is extremely sensitive to TH titer.

The opercle (op), preopercle (pop), subopercle (sop), and interopercle (iop) are all dermal NCC-derived bone. In WT, the bones within the opercular series (which cover the gills) sit flush to one another and are fully ossified (Fig. 5A). The interopercle has a narrow, pointed anterior and wider posterior and is overlapped by the preopercle dorsally and subopercle and opercle posteriorly. The opercle is trapezoidal and slightly concave medially, with the ventral portion of this bone overlapping the sub-opercle. The preopercle is crescent shaped. The sub-opercle is a flat rectangular shape with a pointed anterodorsal corner and the other

edges rounded. In TH –, the opercular series is smaller and overlap of the bones is less pronounced. Importantly, the bones in the opercular series flex noticeably under (qualitatively assessed) pressure, indicating that they are likely not well mineralized (Fig. 5E). The posterodorsal curve of the opercle is also more pronounced, giving it more of a triangular than trapezoidal shape, while the remaining bones of the opercular series do not overlap as in WT suggesting that these bones do not grow to the proper size (Fig. 5E, black box). In TH+, all the bones in the opercular series are oversized and lack the straighter edges of WT (Fig. 5I box; note the uneven edge of the subopercle and the overgrowth in the opercle).

The elements of the lower jaw are both dermal and endochondral NCC-derived bone. The paired anguloarticular, coronomeckelian, dentary, and retroarticular make up the lower jaw (Fig. 5A,B). In TH−, the dentary (d) is often sufficiently shortened that it does not meet the premaxilla properly. Moreover, in older adults, the dentary develops a large ossified growth at the mandibular symphysis, which indicates that TH likely plays a role in proper maintenance of bone (Fig. 5E, observe the dentary, and F, the circle surrounds the unusual bony outgrowth at the symphysis). In addition, the anguloarticular and retroarticular are smaller than that in WT. In TH+, the dentary grows abnormally, with a greatly elongated lower jaw protruding past the upper jaws (Fig. 5I,J). The anguloarticular and retroarticular are larger and more robust than that in WT.

The paired ectopterygoids, metapterygoids (mpt), and entopterygoids (ent) are dermal NCC-derived bones while the paired quadrates (q), sympletics, and hyomandibulae (hm) are endochondral NCC-derived bones. Together these elements support the jaws. In WT, they have cartilaginous junctions (Fig. 5A). In TH−, the cartilaginous junctions are more pronounced (Fig. 5E). In TH+, the cartilaginous junctions are less pronounced (Fig. 5I).

Infraorbitals 1–5 and the supraorbital are dermal NCC-derived bones. In WT, the infraorbital series is made up of irregularly shaped convex ossifications around the ventral portion of the eye while the infraorbital series is a convex bone that sits dorsally to the eye. In TH−, the infraorbital series is generally smaller, and occasionally either infraorbital 1 or 5 is missing. The supraorbital is smaller and often has holes present. In TH+, the infraorbital series and supraorbital show no morphological changes.

To see if TH affected cellular structure in the jaws, and to more closely examine the bony outgrowth of the TH+ dentary, we examined histological sections of all three conditions (Fig. 6). In WT, the ascending process of the premaxilla is well ossified. The kinethmoid is immediately ventral to the premaxilla (Fig. 6A) and is also a solid well-ossified structure. The bones of the upper jaw are surrounded by a combination of fat cells (fc) and disorganized connective tissue (ct), with an overlying thick epithelium (ec) studded with mucus-producing goblet cells (Fig. 6A). The dentary is also fully ossified (Fig. 6D). The intermandibularis muscle (im) is present between the two dentaries and is covered by a layer of fat cells and more disorganized connective tissue. The connective tissue normally found on the rostral extreme of the dentary (Fig. 6D) appears to give rise to the cartilage and bone that make up the bulk of the ectopic ossification seen in older TH− zebrafish.

In TH−, the ascending process of the premaxilla and the kinethmoid maintain the same overall architecture but the cellular structure of these skeletal elements is markedly different from that in WT. The premaxilla is thicker and more curved. The kinethmoid shows differences in several aspects associated with ossification. One end of this median element remains largely cartilaginous. Moreover, instead of being one solid ossified element, the kinethmoid has two ossified ends held together by a sliver of bone, an architecture that is unlikely to be functional (Fig. 6B). There were very few fat cells surrounding the upper jaw of TH− compared with WT, with more of the disorganized connective tissue surrounding it instead (Fig. 6B; note the lack of fat cells dorsal to the premaxilla and connective tissue that fills that space instead). There are fewer mucus-producing goblet cells present and the epithelial layer is overall thinner (compare Fig. 6A,B). Within older TH− fish, there is an additional ossification at the mandibular symphysis (Fig. 6E box and inset). This additional ossification appears to be an endochondral ossification arising from the connective tissue surrounding the dermal dentary, rather than from the dentary itself, and has given rise to chondrocytes and ossified tissue (Fig. 6E inset). As in the upper jaw, there are far fewer mucus-producing goblet cells present.

In TH+, the spatial relationship between the ascending process of the premaxilla and the kinethmoid is retained; however, the histological structure of these two elements suggests that they may contain more mineral in TH+. There are also significantly more fat cells around the upper jaw, resulting in less disorganized connective tissue when compared with WT (Fig. 6C). The TH+ upper jaw is covered in a layer of epithelium that is not studded with mucus-producing goblet cells (Fig. 6A vs. 6C).

In TH+, the dentary is larger than that in WT and fattier in comparison with WT. However, the dentary appears to have ossified correctly (Fig. 6F). The intermandibularis muscle is also larger than that in WT, with the intermandibularis and dentary surrounded in turn by fat cells and a comparatively smaller amount of connective tissue (Fig. 6F; compare the size of the intermandibularis muscle in TH+ with WT). While covered in a layer of squamous epithelium, there are very few mucus-producing goblet cells (Fig. 6F).

Axial Skeleton

The remainder of the axial skeleton is composed of: (1) pelvic, dorsal, anal, and caudal fins with their associated elements, (2) precaudal vertebrae and associated ribs, neural arches, and spines, (3) caudal vertebrae and their associated neural and hemal arches and spines, and (4) intermuscular bones in each myotome (Fig. 7A).

The axial skeleton is composed of mesodermally derived bone (Fig. 7A). The vertebrae ossify around the notochord as dermal bone. The precaudal vertebrae have endochondral neural arches and spines, while the caudal vertebrae have dermal neural arches and spines. In WT, the neural arches have a medial fusion and neural spine (ns) that extends from the point of fusion on both precaudal and caudal vertebral elements. The hemal arches and spines (hs) on the caudal vertebrae are also dermal, except on the preural vertebrae. The hemal arches and spines also have a medial fusion from which the spine extends. The ribs (r) are curved, rod-shaped dermal bone.

In TH−, although the precaudal neural arches and spines are endochondral and the caudal neural and hemal arches and spines are dermal, they exhibit the same types of deformities (Fig. 7B'). The neural and hemal arches and spines generally display patterning issues exemplified by ossified projections but occasionally the two sides of the arches fail to unite and fuse (Fig. 7B'; note the secondary projections emerging from the endochondral neural arch). The neural and hemal spines as well as the ribs lack structural rigidity (Fig. 7B'; compare TH− with WT). In general, the neural and hemal arches and spines, and the pre-, post-, and parazygapophyses are smaller, and the ribs are thinner in TH− than that in WT counterparts (Fig. 7B).

In TH+, the neural and hemal arches and spines are generally larger and more robust (see ns in Fig. 7A' vs. C'), and the anterior most neural arches and spines are long enough that they nearly reach the surface of the skin. The neural and hemal arches and spines as well as the ribs also lack structural rigidity, resulting in a crooked appearance (Fig. 7C; observe the ribs).

The pelvic girdle, dorsal, and anal fins are composed of endochondral bones. The pelvic fin (pf) is composed of the basipterygia and radials that support the lepidotrichia (Fig. 7A). The dorsal and anal fins (df and af, respectively) are both composed of proximal radials, distal radials, and the lepidotrichia (Fig. 7A). In WT, the basipterygium is a flat rodlike process that usually bifurcates anteriorly with a medial posterior curved ischiac process (Fig. 7A). The three radials generally ossify completely, with the medial most radial having a long ossified posterior process and a shorter lateral one. In TH−, the basipterygia of the pelvic girdle remains cartilaginous at the anterior and posterior most tips as well as at the ischiac process (Fig. 7B). The radials generally fail to ossify (Fig. 7B). In TH+, the ischiac process and the posterior rim of the pelvic girdle remains slightly cartilaginous, while the radials generally ossify completely (Fig. 7C).

In WT, the proximal radials of the anal and dorsal fins are flat and bladelike and reach the hemal and neural spines, respectively, with cartilaginous tips seen in some specimens, while the distal radials generally ossify completely (Fig. 7A"). In TH−, proximal radials of the dorsal and anal fins remain cartilaginous at the proximal-most and distal-most tips, while distal radials of the dorsal and anal fins fail to ossify (Fig. 7B"; compare the blue in TH− with WT). In addition, the proximal radials usually fail to interdigitate as thoroughly with the neural/hemal spines (Fig. 7B"; observe the anterior portion of the anal fin and the close-set proximal radials as compared with WT). No morphological changes of the anal or dorsal fin elements were observed in TH+ (Fig. 7C").

The supraneurals (sn) not associated with the Weberian apparatus are endochondral bones that range in number from 4 to 6, with an average of 5, and sit anterior to the neural spines of vertebrae 5–9. In WT, the supraneurals are irregularly shaped but are mostly ossified (Fig. 7A"; observe there are five supraneurals). In TH−, there are generally five or more supraneurals, and the supraneurals are usually smaller and more cartilaginous than in WT (Fig. 7B"; observe that there six supraneurals present). In TH+, all supraneurals were larger and fully ossified, and most TH+ zebrafish examined had five supraneurals (Fig. 7C'; observe that there are five supraneurals).

In WT, the intermuscular bones (im) are dermal ossifications that are embedded within myomeres. In TH−, the intermusculars are usually larger in comparison with WT, and can ossify with secondary projections in TH− zebrafish (Fig. 7B”). In TH+, the intermusculars do not seem to be affected by excess TH (Fig. 7C”).

The caudal fin elements are derived from both dermal and endochondral bone. In TH−, the preurals and uro-style’s neural and hemal arches/spines show defects as stated above in the description of other neural and hemal arches/spines (Fig. 7B). In TH+, the caudal fin elements generally are larger and more robust than in WT, as are the neural and hemal arches and spines (Fig. 7C). All elements of the caudal fin in TH+ also lack the structural rigidity seen in WT and appear wavy.

Patterns of TH Bone Sensitivity

We tested whether the same bones were sensitive to both TH+ and TH− conditions, and whether changes in ossification due to altered TH titer were associated with shape changes as well. We did find that the same bones tended to be affected in both TH+ and TH− conditions (likewise, the same bones tended to be insensitive to TH changes), although the strength of the correlation is relatively low (Supplementary Table S1). Further, bones tended to be affected in both ossification and shape, although again the correlation was significant, but weak. Two bones stood out as particularly sensitive to TH titer: the shape and ossification of both the dentary and ceratobranchial 5 were severely affected in both TH− and TH+ conditions.

In order to identify global patterns in TH sensitivity, we used ordinal logistic regression models including location (craniofacial vs. axial), developmental origin (germ layer; dermal *vs* endochondral), and size at ossification (SL at the onset of ossification). We found that size at ossification was a significant predictor for shape affectedness in both TH− ($P < 0.005$; Fig. 8B”) and TH+ ($P < 0.002$; Fig. 9B”) conditions (see Supplementary Table S1): bones that begin ossification earlier are more likely to show severe shape changes under altered TH profiles. In addition, endochondral bones ($P < 0.0001$) and craniofacial bones ($P < 0.005$) were somewhat more likely to have ossification defects than dermal and axial bones in TH− (Fig. 8; Supporting Information Fig. S1A; Supporting Information Table S1).

Finally, to test for sensitivity to TH in different types of craniofacial bones, we used a model that included information on whether bones were cellular, compact, tubular, and/or spongy (after Weigele and Franz-Odendaal, 2016). The tubular vs. nontubular comparison was dropped from the model because of rank-deficiency and collinearity. Only two factors showed significance: cellular bones ($P = 0.0011$) were more likely to have shape defects under TH− conditions, and spongy bones ($P < <0.0001$) tended to have milder shape defects under TH+ conditions (see Supporting Information Fig. S1 and Supporting Information Table S1). The latter result should be interpreted with caution because of the small sample size of spongy bones in the skull.

DISCUSSION

We found that TH regulates patterning and ossification across anatomical regions and types of bones in the zebrafish skeleton. Developmental hypothyroidism (TH−) causes much more severe defects to overall ossification and patterning, while developmental hyperthyroidism (TH+) results in overossification of numerous elements. Certain structures are particularly sensitive to TH titer: the pectoral girdle, dermatocranium, Weberian apparatus, and dentary show notable defects under abnormal developmental TH profiles.

TH Effects on Different Bone Types

We tested several hypotheses to detect any patterns in types of bones that showed sensitivity to TH, and we were able to detect a few significant correlations. Indeed, we found that endochondral bones were slightly more prone to ossification defects (Fig. 8B'), and early ossifying bones were slightly more prone to shape defects in TH− skeletons (Fig. 8B"). However, while statistically significant, these correlations were quite weak (see Supporting Information Table S1). In general, there were no developmental or categorical features of bones that had real predictive power to tell whether the bone would be sensitive to TH status during development. In all, TH appears to affect all different types of bones, regardless of origin or developmental profile, and sensitivities of specific bones depend on individual characteristics not captured in our categories. Local expression of TH receptors and deiodinases likely determines the sensitivity of individual bones to TH.

TH as an Inhibitor of Ectopic Skeletogenesis

We found that large TH− individuals showed ectopic endochondral bone growth at the mandibular symphysis. This ectopic ossification appears to originate from the connective tissue rostral to the dentary, indicating that the overall maintenance of bone and connective tissue in that area has been disrupted. Heterotopic bone formation is usually associated with metastases of cancer cells, injury, and illness such as pseudoparahypothyroidism (Levine, 2012; Takeda et al., 2013). However, this late adult shift from disorganized connective tissue to endochondral bone is not typical of hypothyroidism in mouse models or in humans. Thus, we posit that TH plays a role in the maintenance of this particular connective tissue. Furthermore, we found that both the postcleithrum and neural and hemal arches and spines display ectopic ossifications in TH− zebrafish, indicating that TH plays a role in proper patterning of ossification.

Comparison of Our Results With Previous Analyses of Hyper/Hypothyroidism in Fishes

Our anatomical results are largely consistent with previous studies of induced TH− and TH+ conditions, although there are key differences (Shkil and Smirnov, 2008; Shkil et al., 2010a,b; Shkil et al., 2012; Smirnov et al., 2012; Kapitanova and Shkil, 2014a,b). Our work uses zebrafish that have endogenously altered TH levels (McMenamin et al., 2014) rather than exogenously altered TH levels by continuous drug treatments (Shkil et al., 2012; Kapitanova and Shkil, 2014a). In the exogenous system, zebrafish are treated with T3 and the goitrogen thiourea, and this exogenous treatment produces extreme phenotypes that are not recapitulated in our endogenous system (Shkil et al., 2012; Kapitanova and Shkil, 2014a,b).

The intercalarium showed severe defects in Kapitanova and Shkil (2014b), with the hyperthyroid fish producing an ovaloid bone that lacked both an ascending process and the manubrium and had no clear articular process, while the hypothyroid fish produced an extremely wide and twisted manubrium that split at the tip with a more robust ascending process. However, we observed that both our TH− and TH+ zebrafish had a clearly defined articular process, manubrium, and ascending process. Some of these differences may be due to off-target effects of drug treatments, or could stem from residual TH production in our TH − fish.

Comparison of Zebrafish and Mouse Models

Many of the defects observed in our TH-modulated zebrafish are similar to changes seen in mice. For example, in our TH− adult zebrafish, a fontanelle is present where the frontals and parietals normally fuse. In neonatal mice, although there is already a fontanelle where the frontals and parietals should ultimately meet, it is substantially enlarged compared with the WT condition as seen in a number of different hypothyroid mouse lineages including *Pax8*$^{-/-}$ and *TRa*$^{R384C/+}$ (Stein et al., 1994; Bassett et al., 2007; Bassett and Williams, 2016). In addition, like our TH− zebrafish, hypothyroid mouse models (including *Pax8*$^{-/-}$ and *Hyt/Hyt)* show an overall smaller stature and lack proper dermal and endochondral ossification (Stein et al., 1994; Bassett and Williams, 2016). In TH+ zebrafish, the overlap of the frontal and parietal sutures is more robust than that in WT. This is consistent with results from hyperthyroid mouse models, which show early fusion/ossification of a number of bones, including craniosynostosis of the braincase (Forrest et al., 1996; Gauthier et al., 2001; Bassett et al., 2007; Bassett and Williams, 2016). The shared anatomical defects between the zebrafish and mouse models demonstrate that the zebrafish TH-manipulation hyperthyroid models will allow us to augment our understanding of the role of TH in skeletogenesis.

Functional Consequences

The skeletal changes seen in TH-modulated fish likely result in functional consequences. Indeed, TH is required for the onset of mature feeding behaviors, and the failure of elements such as the kinethmoid and premaxilla to properly ossify may help explain the lack of premaxillary protrusion in TH− adults (McMenamin et al., 2017; Galindo et al., 2018). In particular, the kinethmoid is a sesamoid bone and as such is dependent on proper functioning of upper jaw protrusion to properly ossify. In TH− fish, the kinethmoid is thin and underossified, and one end of the bone remains cartilaginous (Figs. 5H and6B); these differences may preclude normal upper jaw protrusion. The disruptions in tooth size and number likely also result in functional consequences during food processing, since zebrafish lack oral teeth and a stomach, relying on the pharyngeal jaws for all food processing (Hernandez et al., 2007).

The Weberian apparatus showed considerable sensitivity to TH status. The bones of the Weberian apparatus are modified ribs and vertebrae that connect the swim bladder to the inner ear (functionally analogous to the mammalian middle ear). Thus, it seems likely that TH-disrupted fish have hearing defects. Furthermore, hypothyroidism is associated with hearing loss in mammals, and TH is required for proper development of the cochlea (Deol, 1973; Uziel et al., 1981; Knipper et al., 2001; Rusch et al., 2001; Ng et al., 2009). The bones

of the middle ear pass vibrations from the tympanic membrane to the inner ear, but roles of TH in the development of the middle ear have received less research attention (although hypothyroid mice show increased size and decreased ossification in middle ear ossicles; Cordas et al., 2012). The mammalian stapes, incus, and malleus are homologous to the hyomandibula, quadrate, and articular in fish. We found that the hyomandibula and quadrate have more cartilaginous junctions in TH− and are more ossified in TH+ than in WT. The articular is dermal bone, and is smaller in TH− and larger in TH+. Close study of these elements in zebrafish may be a useful tool for studying the effects of TH on development of their mammalian homologues and, ultimately, hearing. Thus, zebrafish may be a useful tool to further our understanding of how TH supports the development of hearing from skeletal and functional perspectives.

Supplementary Material

Refer to Web version on PubMed Central for supplementary material.

ACKNOWLEDGMENTS

The authors wish to thank all the members of the Hernandez and McMenamin labs for their support and productive discussions. We thank W. James Cooper and another anonymous reviewer for constructive comments. Special thanks to Angela Mauri in the McMenamin lab for help with illustrations. The research was supported by NIH grants R03HD091634 (to SKM and LpH) and R00GM105874 (to SKM), and Burroughs Wellcome Fund Collaborative Research Travel Grant 1017493 (to SKM).

Grant sponsor: Burroughs Wellcome Fund; Grant number: Collaborative Research Travel Grant 1017493; Grant sponsor: Eunice Kennedy Shriver National Institute of Child Health and Human Development; Grant number: R03HD091634; Grant sponsor: National Institutes of Health; Grant number: R00GM105874.

LITERATURE CITED

Allain TJ, McGregor AM. 1993 Thyroid hormones and bone. J Endocrinol 139:1399–1318.

Bassett JHD, Nordström K, Boyde A, Howell PGT, Kelly S, Vennström B, Williams GR. 2007 Thyroid status during skeletal development determines adult bone structure and mineralization. Mol Endocrinol 21:1893–1904. [PubMed: 17488972]

Bassett JDH, Williams GR. 2016 Role of thyroid hormones in skeletal development and bone maintenance. Endocr Rev 37:135–187. [PubMed: 26862888]

Bird NC, Hernandez LP. 2007 Morphological variation in the Weberian apparatus of Cypriniformes. J Morphol 268:739–757. [PubMed: 17591731]

Bird NC, Mabee PM. 2003 Developmental morphology of the axial skeleton of the zebrafish, Danio rerio (Ostariophysi: Cyprinidae). Dev Dyn 228:337–357. [PubMed: 14579374]

Cordas EA, Ng L, Hernandez A, Kaneshige M, Cheng SY, Forrest D. 2012 Thyroid hormone receptors control developmental maturation of the middle ear and the size of the ossicular bones. Endocrinology 153:1548–1560. [PubMed: 22253431]

Cubbage CC, Mabee PM. 1996 Development of the cranium and paired fins in the zebrafish Danio rerio (Ostariophysi, Cyprinidae). J Morphol 229:121–160. [PubMed: 29852585]

De Leo S, Lee SY, Braverman LE. 2016 Hyperthyroidism. Lancet 388:906–918. [PubMed: 27038492]

Deol MS. 1973 Congenital deafness and hypothyroidism. Lancet 2: 105–106.

Devdhar M, Ousman YH, Burman KD. 2007 Hypothyroidism. Endocrinol Metab Clin North Am 36:595–615. [PubMed: 17673121]

Ducy P, Zhang R, Geoffroy V, Ridall AL, Karsenty G. 1997 Osf2/Cbfa1: a transcriptional activator of osteoblast differentiation. Cell 89:747–754. [PubMed: 9182762]

Fratzl-Zelman N, Hörandner H, Luegmayr E, Varga F, Ellinger A, Erlee MPM, Klaushofer K. 1997 Effects of triiodothyronine on the morphology of cells and matrix, the localization of alkaline phosphatase, and the frequency of apoptosis in long-term cultures of MC3T3-E1 cells. Bone 20:225–236. [PubMed: 9071473]

Forrest D, Hanebuth E, Smeyne RJ, Everds N, Stewart CL, Wehner JM, Curran T. 1996 Recessive resistance to thyroid hormone in mice lacking thyroid hormone receptor beta: evidence for tissue-specific modulation of receptor function. EMBO J 15(12): 3006–3015. [PubMed: 8670802]

Galindo D, Sweet S, DeLeon Z, Wagner M, DeLeon A, Carter C, McMenamin S, Cooper WJ. 2018 Thyroid hormone modulation during zebrafish development recapitulates evolved diversity in danionin jaw protrusion mechanics. bioRxiv preprint. 10.1101/418483.

Gauthier K, Plateroti M, Harvey CB, Williams GR, Weiss RE, Refetoff S, Willott JF, Sundin V, Roux JP, Malaval L, et al. 2001 Genetic analysis reveals different functions for the products of the thyroid hormone receptor alpha locus. Mol Cell Biol 21(14): 4748–4760. [PubMed: 11416150]

Gouveia C 2001 Thyroid hormone stimulation of osteocalcin gene expression in ROS 17/2.8 cells is mediated by transcriptional and post-transcriptional mechanisms. J Endocrinol 170:667–675. [PubMed: 11524248]

Hernandez LP, Bird NC, Staab KL. 2007 Using zebrafish to investigate cypriniform evolutionary novelties: functional development and evolutionary diversification of the kinethmoid. J Exp Zool B Mol Dev Evol 308:625–641. [PubMed: 17358013]

Hernandez LP, Staab KL. 2015 Bottom feeding and beyond: how the premaxillary protrusion of cypriniforms allowed for a novel kind of suction feeding. Integr Comp Biol 55:74–84. [PubMed: 25976909]

Himeno M, Enomoto H, Liu W, Ishizeki K, Nomura S, Kitamura Y, Komori T. 2002 Impaired vascular invasion of Cbfa1-deficient cartilage engrafted in the spleen. J Bone Miner Res 17:1297–1305. [PubMed: 12096844]

Ishikawa Y, Genge BR, Wuthier RE, Wu LNY. 1998 Thyroid hormone inhibits growth and stimulates terminal differentiation of epiphyseal growth plate chondrocytes. J Bone Miner Res 13: 1398–1411. [PubMed: 9738512]

Kapitanova DV, Shkil FN. 2014a Effects of thyroid hormone level alterations on the development of supraneural series in zebrafish, Danio rerio. J App Ichthyol 30:821–824.

Kapitanova DV, Shkil FN. 2014b Effects of thyroid hormone level alterations on the Weberian apparatus ontogeny of cyprinids (Cyprinidae; Teleostei). Russ J Dev Biol 45:313–323.

Knipper M, Richardson G, Mack A, Müller M, Goodyear R, Limberger A, Rohbock K, Köpschall I, Zenner HP, Zimmermann U. 2001 Thyroid hormone-deficient period prior to the onset of hearing is associated with reduced levels of β-tectorin protein in the tectorial membrane. J Biol Chem 276:39046–39052. [PubMed: 11489885]

Klaushofer K, Hoffmann O, Gleispach H, Leis HJ, Czerwenka E, Koller E, Peterlik M. 1989 Bone-resorbing activity of thyroid hormones is related to prostaglandin production in cultured neonatal mouse calvaria. J Bone Miner Res 4:305–312. [PubMed: 2504036]

Kronenberg HM. 2003 Developmental regulation of the growth plate. Nature 423:332–336. [PubMed: 12748651]

Lassova L, Niu Z, Golden EB, Cohen AJ, Adams SL. 2009 Thyroid hormone treatment of cultured chondrocytes mimics in vivo stimulation of collagen X MRNA by increasing BMP 4 expression. J Cell Physiol 219:595–605. [PubMed: 19170125]

Levine MA. 2012 An update on the clinical and molecular characteristics of pseudohypoparathyroidism. Curr Opin Endocrinol Diabetes Obes 19:443–451. [PubMed: 23076042]

Makihira S, Yan W, Murakami H, Furukawa M, Kawai T, Nikawa H, Yoshida E, Hamada T, Okada Y, Kato Y. 2003 Thyroid hormone enhances aggrecanase-2/ADAM-TS5 expression and proteoglycan degradation in growth plate cartilage. Endocrinology 144: 2480–2488. [PubMed: 12746310]

McMenamin SK, Bain EJ, McCann AE, Patterson LB, Eom DS, Waller ZP, Hamill JC, Kuhlman JA, Eisen JS, Parichy DM. 2014 Thyroid hormone–dependent adult pigment cell lineage and pattern in zebrafish. Science 345:1358–1361. [PubMed: 25170046]

McMenamin SK, Carter C, Cooper WJ. 2017 Thyroid hormone stimulates the onset of adult feeding kinematics in zebrafish. Zebrafish 14:517–525. [PubMed: 28933679]

Miura M, Tanaka K, Komatsu Y, Suda M, Yasoda A, Sakuma Y, Ozasa A, Nakao K. 2002 Thyroid hormones promote chondrocyte differentiation in mouse ATDC5 cells and stimulate endochondral ossification in fetal mouse tibias through iodothyronine deiodinases in the growth plate. J Bone Miner Res 17:443–454. [PubMed: 11874236]

Mundy GR, Shapiro JL, Bandelin JG, Canalis EM, Raisz LG. 1976 Direct stimulation of bone resorption by thyroid hormones. J Clin Invest 58:529–534. [PubMed: 182721]

Nelson JS. 2006 Fishes of the World. 4th ed. Hoboken, NJ: John Wiley & Sons.

Ng L, Hernandez A, He W, Ren T, Srinivas M, Ma M, Galton VA, St. Germain DL, Forrest D. 2009 A protective role for type 3 deiodinase, a thyroid hormone-inactivating enzyme, in cochlear development and auditory function. Endocrinology 150:1952–1960. [PubMed: 19095741]

O'Shea PJ, Kim DW, Logan JG, Davis S, Walker RL, Meltzer PS, Cheng SY, Williams GR. 2012 Advanced bone formation in mice with a dominant-negative mutation in the thyroid hormone receptor β gene due to activation of Wnt/ß-catenin protein signaling. J Biol Chem 287:17812–17822. [PubMed: 22442145]

Persani L 2012 Clinical review: central hypothyroidism: pathogenic, diagnostic, and therapeutic challenges. J Clin Endocrinol Metabol 97:3068–3078.

Robson H, Siebler T, Stevens DA, Shalet SM, Williams GR. 2000 Thyroid hormone acts directly on growth plate chondrocytes to promote hypertrophic differentiation and inhibit clonal expansion and cell proliferation. Endocrinology 141:11.

Rusch A, Ng L, Goodyear R, Oliver D, Lisoukov I, Vennström B, Richardson G, Kelley MW, Forrest D. 2001 Retardation of cochlear maturation and impaired hair cell function caused by deletion of all known thyroid hormone receptors. J Neurosci 21:9792–9800. [PubMed: 11739587]

Shkil FN, Smirnov SV. 2008 Thyroid Responsiveness of the large African barb Labeobarbus intermedius (Teleostei; Cyprinidae): individual variability and morphological consequences. Dokl Biol Sci 425:144–146.

Shkil FN, Borisov VB, Smirnov SV. 2010a Influence of thyroid hormone on the sequence of cranial bones appearance in early ontogeny of the large African barb (Labeobarbus intermedius; Cyprinidae; Teleostei). Dokl Biol Sci 432:224–226. [PubMed: 20665160]

Shkil FN, Abdissa B, Smirnov SV. 2010b Role of thyroid hormone in the ontogeny and morphological diversification of Barbus intermedius sensu Banister, 1973 of Lake Tana in Ethiopia. Russ J Dev Biol 41:369–380.

Shkil FN, Kapitanova DV, Borisov VB, Abdissa B, Smirnov SV. 2012 Thyroid hormone in skeletal development of cyprinids: effects and morphological consequences. J App Ichthyol 28:398–405.

Smirnov SV, Kapitanova DV, Borisov VB, Abdissa B, Shkil FN. 2012 Lake Tana large barbs diversity: developmental and hormonal bases. J Ichthyol 52:861–880.

Stein SA, Oates EL, Hall CR, Grumbles RM, Fernandez LM, Taylor NA, Puett D, Jin S. 1994 Identification of a point mutation in the thyrotropin receptor of the hyt/hyt hypothyroid mouse. Mol Endocrinol 8:129–138. [PubMed: 8170469]

Takeda M, Mikami T, Numata Y, Okamoto M, Okayasu I. 2013 Papillary thyroid carcinoma with heterotopic ossification is a special subtype with extensive progression. Am J Clin Pathol 139: 586–598.

Uziel A, Romand R, Marot M. 1981 Development of cochlear potentials in rats. Audiology 20:89–100. [PubMed: 7224981]

Vestergaard P, Mosekilde L. 2002 Fractures in patients with hyperthyroidism and hypothyroidism: a nationwide follow-up study in 16,249 patients. Thyroid 12:411–419. [PubMed: 12097203]

Vestergaard P, Rejnmark L, Mosekilde L. 2005 Influence of hyper-and hypothyroidism, and the effects of treatment with antithyroid drugs and levothyroxine on fracture risk. Calcif Tissue Int 77: 139–144. [PubMed: 16151671]

Walker MB, Kimmel CB. 2007 A two-color acid-free cartilage and bone stain for zebrafish larvae. Biotech Histochem 82:23–28. [PubMed: 17510811]

Weigele J, Franz-Odendaal TA. 2016 Functional bone histology of zebrafish reveals two types of endochondral ossification, different types of osteoblast clusters and a new bone type. J Anat 229: 92–103. [PubMed: 27278890]

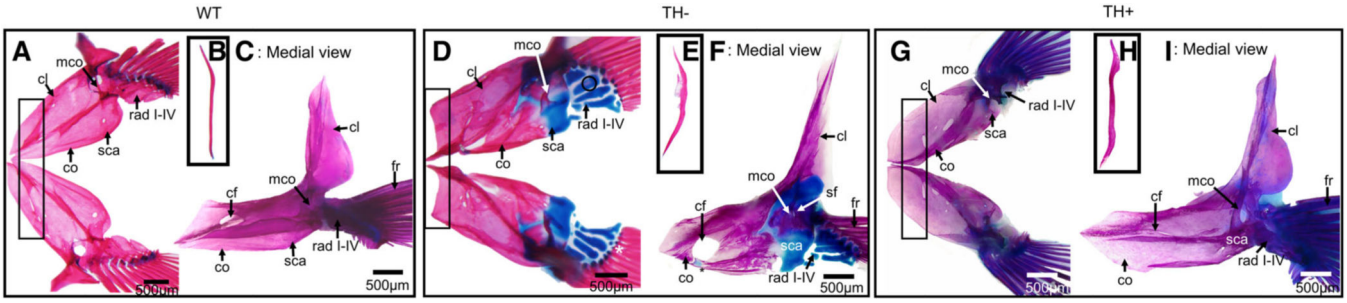

Fig. 1.

Cleared and stained (C&S) pectoral girdle from WT (euthyroid), TH− (hypothyroid), and TH+ (hyperthyroid) zebrafish. Bone is stained with Alizarin red, and cartilage is stained with Alcian blue. Note the overall lack of ossification in TH− and the overossification in TH+. (**A**, **D**, and **G**) Pectoral girdle in dorsal view. Note the lack of the anteroventral curve to the cleithrum in TH− and the more angular curve in TH+ (box). Radials failed to ossify in TH−, with the exception of a very small region on the third proximal radial (circle). (**B**, **E**, and **H**) Postcleithra in medial view. Note the secondary ossifications in TH− and the more robust ossification in TH+. (**C**, **F**, and **I**): Pectoral girdle in medial view. Note that the cleithrum's lateral plate is foreshortened in TH− and more robust in TH+. The coracoid foramen (*cf*) is also larger in TH− and surrounded by traces of cartilage, and smaller in TH+. Abbreviations: *cf*, coracoid foramen; cl, cleithrum; co, coracoid; fr, finrays; mco, mesocoracoid; rad I–IV, radials I–IV; sca, scapula; sf, scapular foramen.

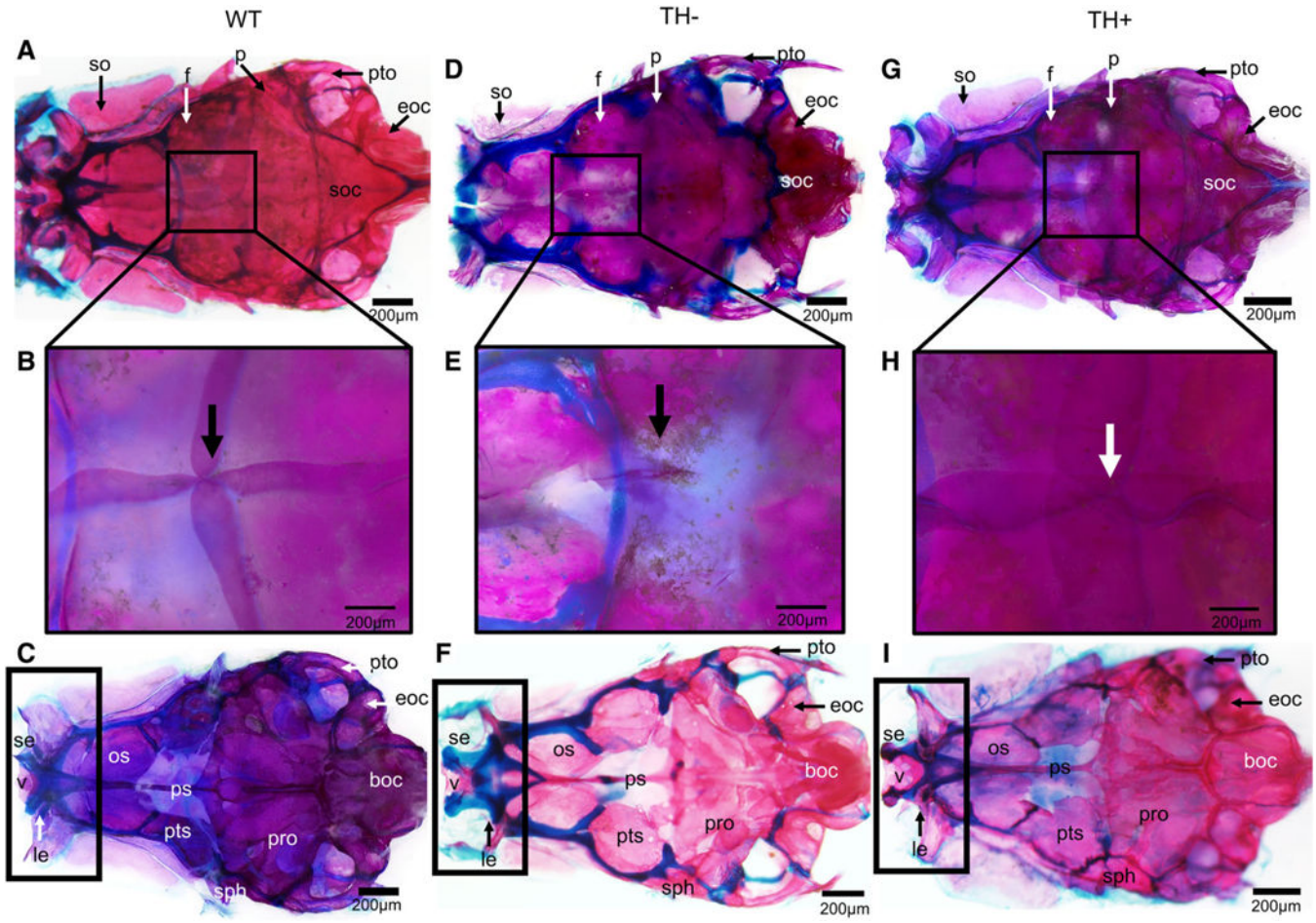

Fig. 2.

Cleared and stained skull from WT, TH−, and TH+ zebrafish. Note the overall lack of ossification in TH− and over-ossification in TH+. (**A**, **D**, and **G**) Dorsal view of the dermatocranium. Black boxes indicate the point of fusion of the frontals and parietals. (**B**, **E**, and **H**) Closeup of dermatocranium showing point of fusion of the frontals and parietals. Note in TH− the open hole where the frontals and parietals should meet, and the more robust fusion in TH+ where the frontals and parietals overlap. (**C**,**F**, and **I**) Ventral view of the neurocranium. Black boxes indicate the rostral portion of the neurocranium, which is considerably more cartilaginous in TH− and considerably less cartilaginous in TH+. Abbreviations: boc, basioccipital; eoc, exoccipital; f, frontal; le, lateral ethmoid; os, orbitosphenoid; p, parietal; ps, parasphenoid; pts, pterosphenoid; pro, prootic; pto, pterotic; se, supraethmoid; sph, sphenotic; so, supraorbital; soc, supraoccipital; v, vomer.

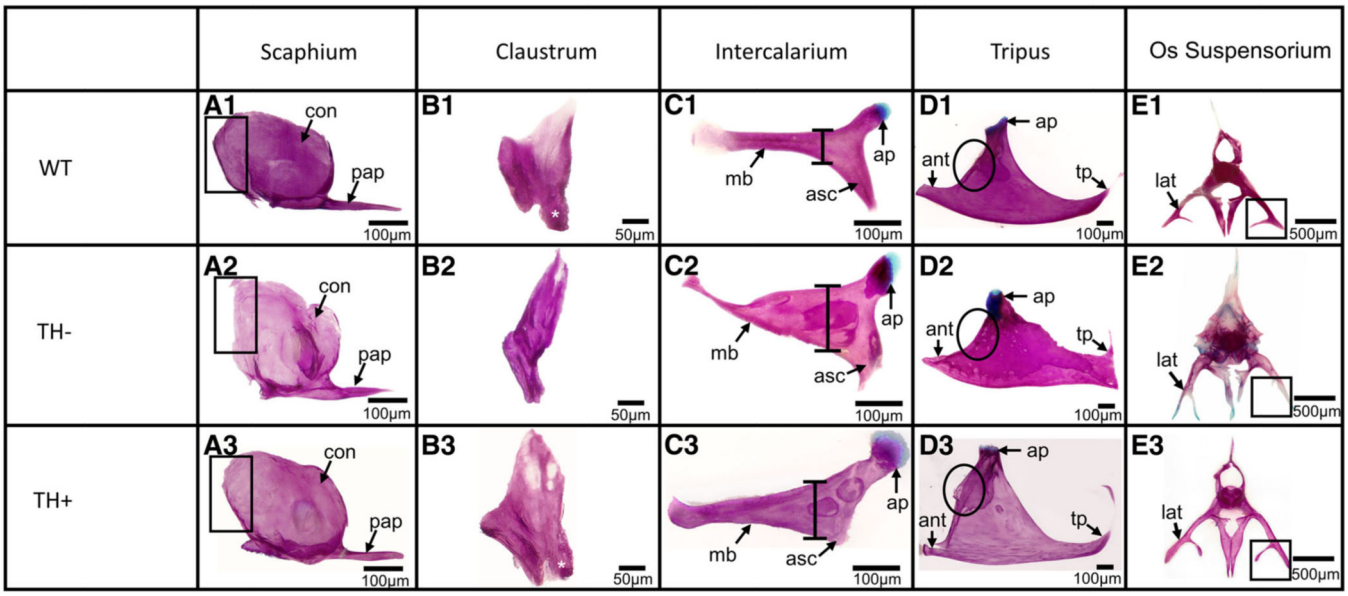

Fig. 3.

Cleared and stained Weberian ossicles from WT, TH−, and TH+ zebrafish. The order of the images **(A-E)** of the Weberian ossicles match their anterior to posterior position within the zebrafish. (A1–3) Scaphium. Note the lack of a properly ossified anterior edge to the concha of the scaphium in TH−. (B1–3) Claustrum. Asterisks indicate the presence of a posterior leg of the claustrum, present in WT and TH+, but absent in TH−. (C1–3) Intercalarium. Bars indicate the widest point of the intercalarium's manubrium. In TH− and TH+, it is enlarged, but the distal end of the manubrium is smaller in TH−. Asterisks mark the ascending process. Note that this process is larger in both TH− and TH+ than in WT but does not extend as far as in WT. (D1–3) Tripus. Arrows indicate the transformator process. Note the oddly shaped transformator process in TH− and the lengthened transformator process in TH +. Note the lack of proper definition of the anterior process in TH− and TH+ (black circles). (E1–3) Os suspensoria. Arrows indicate the lateral arm of the os suspensorium. Note both the underossification in TH− and increased size in TH+.

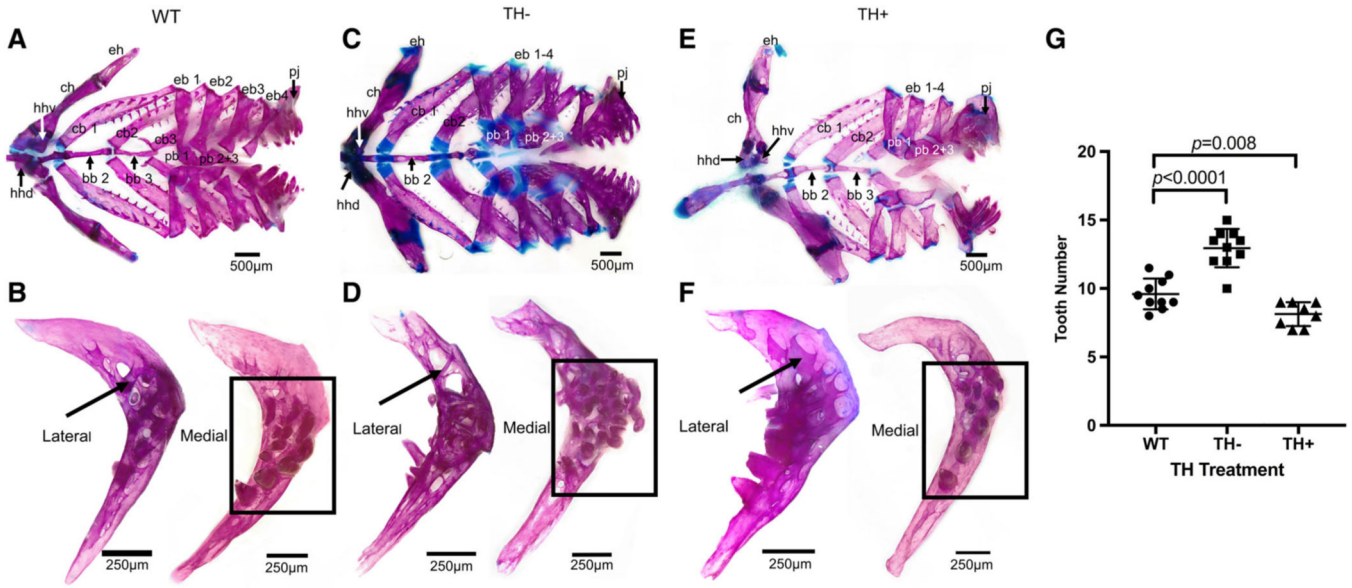

Fig. 4.

Cleared and stained branchial basket from WT, TH−, and TH+ zebrafish. (**A**, **C**, and **E**) Dorsal view of the branchial basket. Note the more prominent cartilaginous junctions in TH −. (**B**, **D**, and **F**) Lateral and medial view of the pharyngeal jaws. Bold arrows indicate the supporting struts of the pharyngeal jaws. Black boxes surround the teeth. (**G**) WT showed between 7 and 12 teeth on each pharyngeal jaw (average = 9.6, N = 10 fish), TH− showed between 9 and 17 (average = 12.95, N = 10 fish) and TH+ showed between 7 and 10 (average = 8.1, N = 8 fish). The presence of TH inhibits pharyngeal teeth, as TH− jaws had significantly more teeth (two tailed t test $P = 1.4e-05$) and TH+ had significantly fewer teeth ($P = 0.0079$) than WT jaws. Further, teeth were more robustly ankylosed to the ceratobranchial in TH+. Abbreviations: bb, basibranchial; cb, ceratobranchial; ch, ceratohyal; eb, epibranchial; eh, epihyal; hhd, hypohyal dorsal; hhv, hypohyal ventral; pb, pharyngobranchial. Bones within a series are labeled with the corresponding numbers (e.g., pb 1, pb 2 + 3).

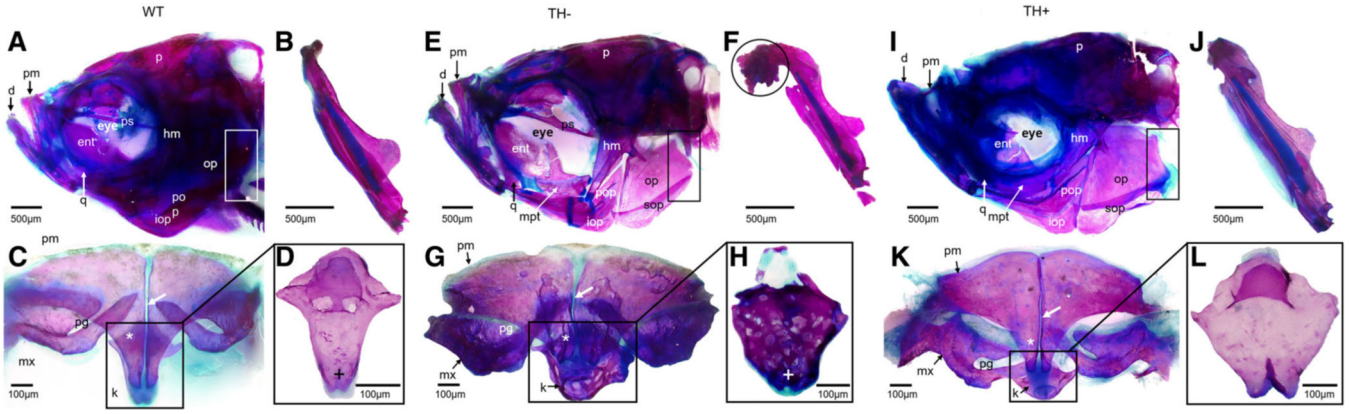

Fig. 5.

Cleared and stained jaw and suspensorium from WT, TH−, and TH+ zebrafish. (**A**, **E**, and **I**) Lateral view of craniofacial features. Note the differences in shape of the operculum, with the dorsal most edge of TH− improperly ossified and the more robust and larger operculum in TH+. (**B**, **F**, and **J**) Dentary. Note the bony process on the mandibular symphysis, which only appears in older adult TH− zebrafish, and the enlarged dentary in TH+. (**C**, **G**, and **K**) Dorsal view of the upper jaw elements. Arrows indicate the symphysis between the premaxillae. Asterisks indicate the ascending process of the premaxilla. Note that the ascending process of the premaxilla fails to form correctly in TH−. The rostral and premaxillary processes of the maxilla also do not form properly in TH−, and so the premaxilla does not sit properly in the groove formed by these two maxillary processes. (**D**, **H**, and **L**) Anterior view of kinethmoids. Note lack of discrete lateral wings, unossified dorsal edge, and trabecular-like bone in the TH−, and the asymmetrical lateral wing formation in TH+. Abbreviations: hm, hyomandibula; k, kinethmoid; mx, maxilla; op, operculum; pg, premaxillary groove; pm, premaxilla.

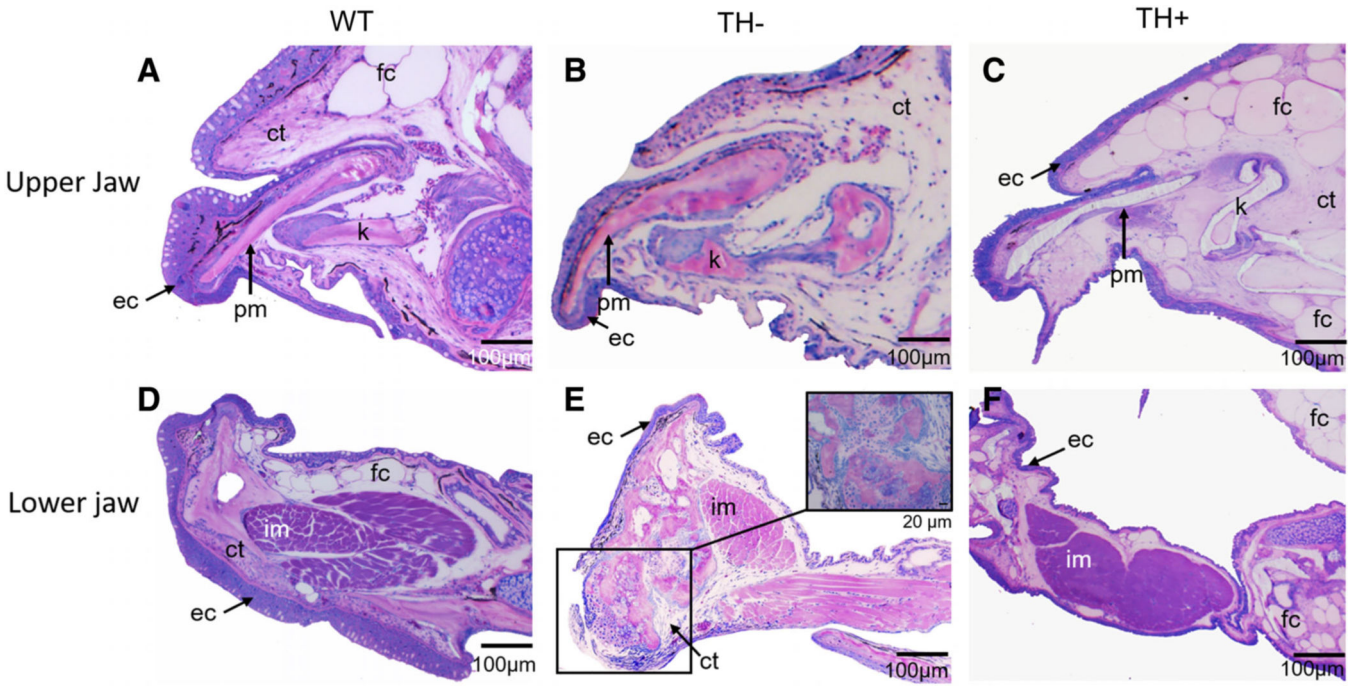

Fig. 6.

Parasagittal sections from WT, TH−, and TH+ zebrafish stained with Lee's Methylene Blue-Basic Fuschin. (**A**, **B**, and **C**) Sections through upper jaw showing histological structure of premaxilla and kinethmoid. (**D**, **E**, and **F**) Sections through lower jaw showing histological structure of dentary and intermandibularis muscle. Note the thin epithelium, lack of fat cells, and disorganized connective tissue in the upper and lower jaw of TH−, and the thin epithelium, surplus of fat cells, and lack of connective tissue in TH+. In TH−, the intermandibularis muscle is smaller than in WT, while in TH+ it is larger. (E, inset) Closeup view of the endochondral bone growth at the tip of the dentary, present only in older TH− individuals.

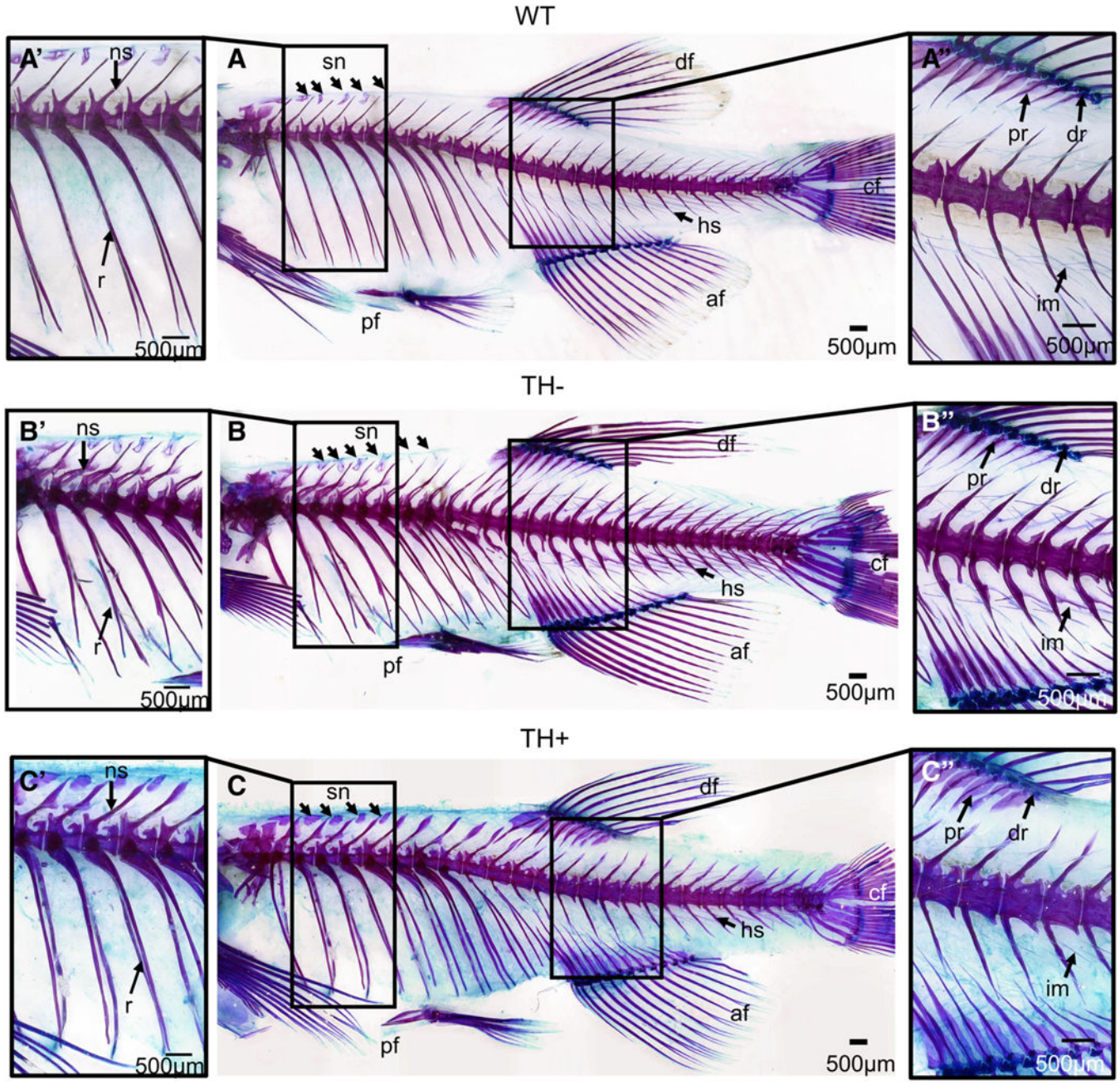

Fig. 7.

Cleared and stained axial skeleton from WT, TH−, and TH+ zebrafish. **(A**, **A**', and **A")** Lateral view of the WT axial skeleton. **(B**, **B**', **B")** Lateral view of the TH− axial skeletal. The TH− skeleton is more compressed on an anterior to posterior axis (B). Note the secondary projections and lack of structural rigidity of the neural and hemal arches and spines (B'). Also note the proximal and distal radials fail to fully ossify (B"). (**C**, **C**', and **C**") Lateral view of the TH+ axial skeleton. The TH+ zebrafish is overall larger on the anterior to posterior axis (C). Note that the neural and hemal arches and spines are larger than that in WT and the anterior most supraneurals broaden instead of narrow at the tip (C').

Abbreviations: af, anal fin; cf, caudal fin; df, dorsal fin; dr, distal radials; hs, hemal spines; ns, neural spines; pf, pelvic fin; pr, proximal radials; sn, supraneural.

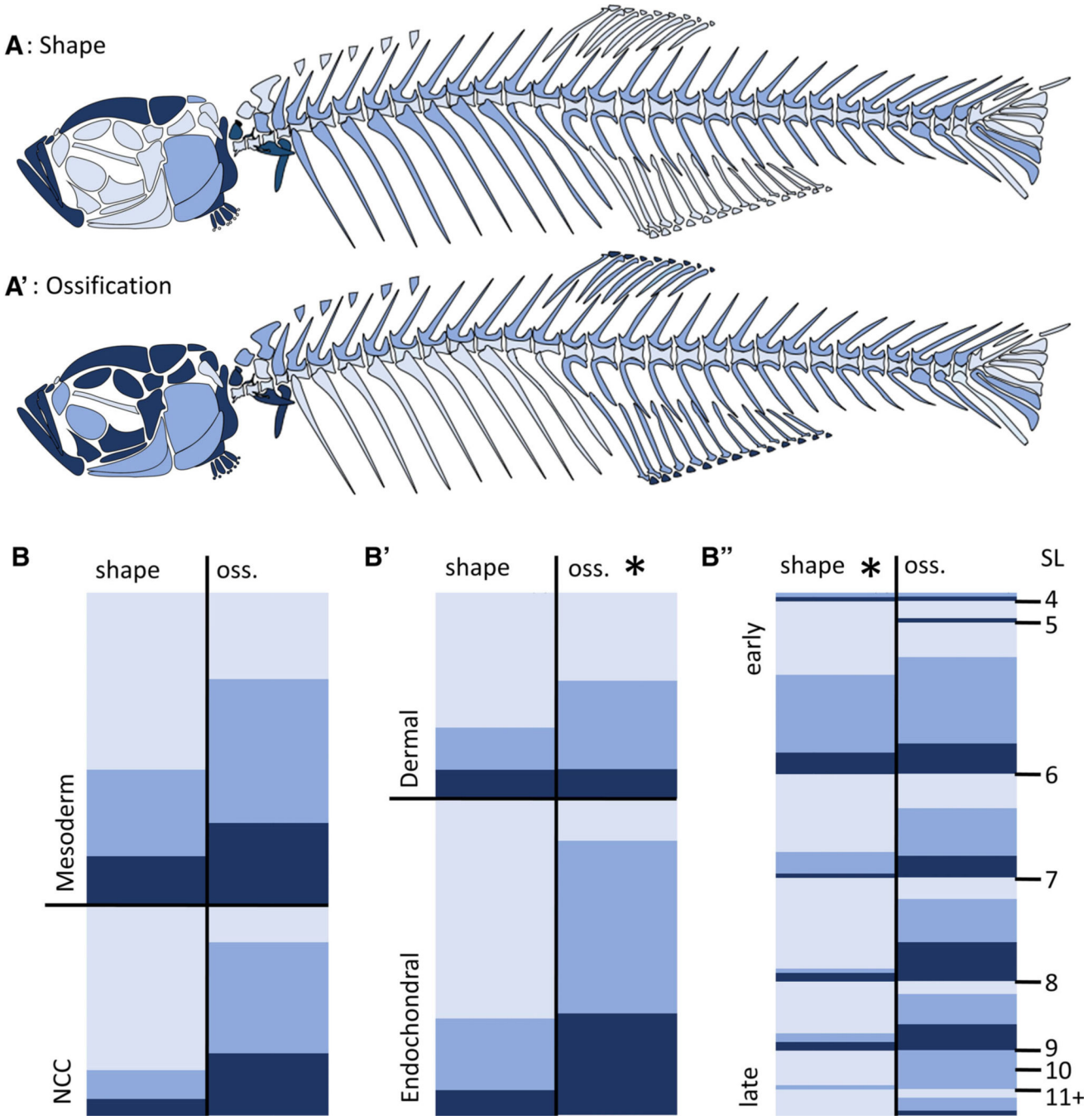

Fig. 8.

Global patterns of bone sensitivity to hypothyroidism (TH−). **(A** and **A')**: Schematics showing bones that do not achieve proper shape (A) or ossification (A') in TH− backgrounds. **(B)** Heat maps show disruption in shape (left) and ossification (oss., right) for each bone sorted by different cellular origins (B, mesoderm vs. NCC), ossification profiles (B', dermal vs. endochondral) and timing of ossification (B"). In (B"), bones are sorted by size range at which they ossify. Asterisks indicate significance within a category as

determined by ordinal logistic regression. Light blue, unaffected; blue, moderately affected; dark blue, severely affected relative to euthyroid.

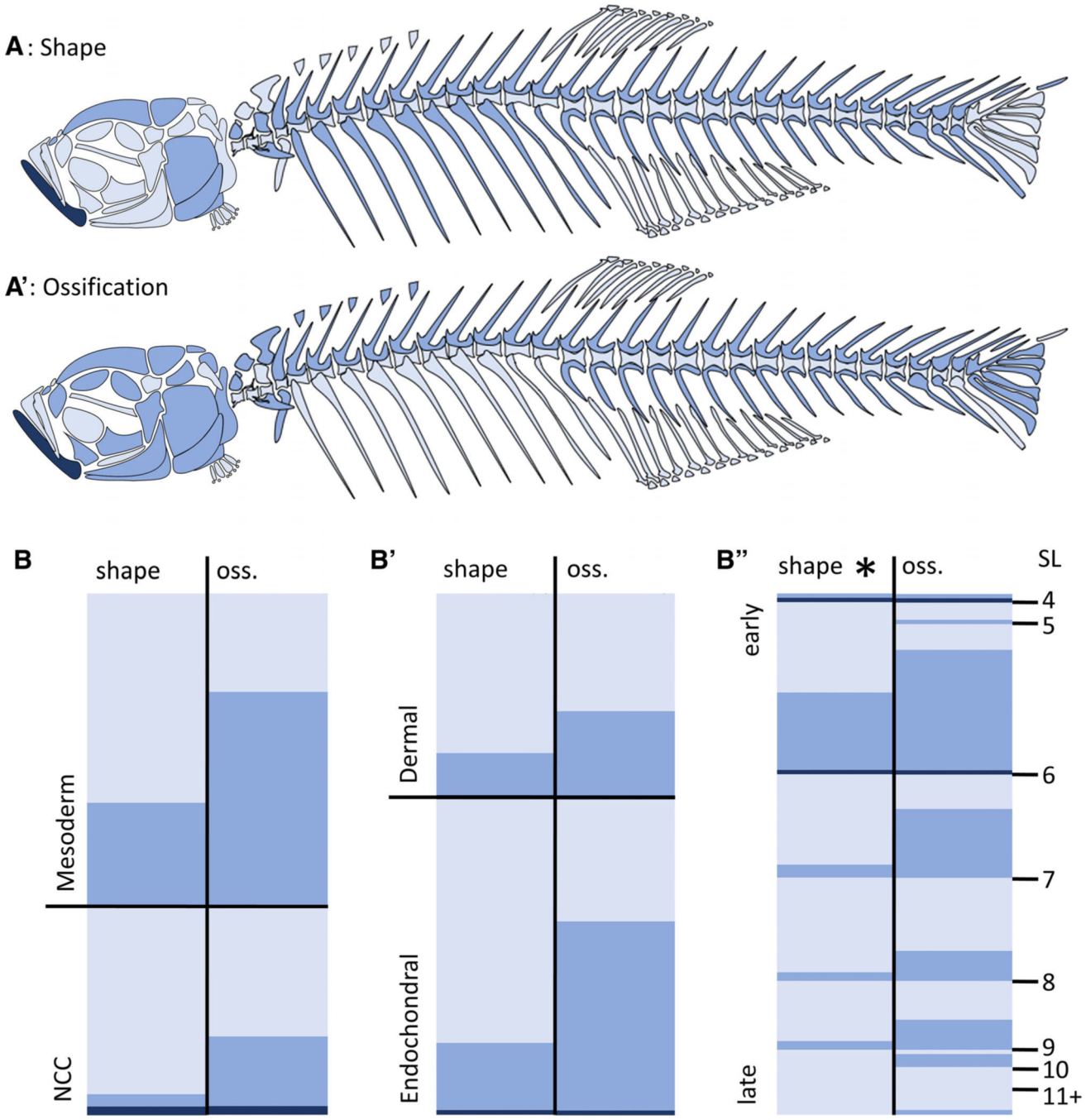

Fig. 9.

Global patterns of bone sensitivity to hyperthyroidism (TH+). **(A** and **A')** Schematics showing bones that do not achieve proper shape (A) or ossification (A') in TH+ backgrounds. **(B)** Heat maps show disruption in shape (left) and ossification (oss., right) for each bone sorted by different cellular origins (B, mesoderm vs. NCC), ossification profiles (B', dermal vs. endochondral) and timing of ossification (B"). In (B"), bones are sorted by size range at which they ossify. Asterisk indicates significance as determined by ordinal

logistic regression. Light blue, unaffected; blue, moderately affected; dark blue, severely affected relative to euthyroid.